



Second-generation corneal deformation signal waveform analysis in normal, forme fruste keratoconic, and manifest keratoconic corneas after statistical correction for potentially confounding factors

Lijun Zhang, MD, PhD, Jennifer Danesh, BS, Anjali Tannan, MD, Vivian Phan, OD, Fei Yu, PhD, D. Rex Hamilton, MD, MS

PURPOSE: To evaluate the difference in corneal biomechanical waveform parameters between manifest keratoconus, forme fruste keratoconus, and healthy eyes with a second-generation biomechanical waveform analyzer (Ocular Response Analyzer 2).

SETTING: Jules Stein Eye Institute, University of California, Los Angeles, California, USA.

DESIGN: Retrospective chart review.

METHODS: The biomechanical waveform analyzer was used to obtain corneal hysteresis (CH), corneal resistance factor (CRF), and 37 biomechanical waveform parameters in manifest keratoconus eyes, forme fruste keratoconus eyes, and healthy eyes. Useful distinguishing parameters were found using *t* tests and a multivariable logistic regression model with stepwise variable selection. Potential confounders were controlled for.

RESULTS: The study included 68 manifest keratoconus eyes, 64 forme fruste keratoconus eyes, and 249 healthy eyes. There was a statistical difference in the mean CRF between the normal group ($10.2 \text{ mm Hg} \pm 1.7 \text{ [SD]}$) and keratoconus group ($6.3 \pm 1.9 \text{ mm Hg}$) ($P = .003$), and between the normal group and the forme fruste keratoconus group ($7.8 \pm 1.4 \text{ mm Hg}$) ($P < .0001$). There was no statistical difference in the mean CH between the normal group and the keratoconus group or the forme fruste keratoconus group. The CRF, height of peak 1 (P1) ($P = .001$), downslope of P1 (dslope1) ($P = .027$), upslope of peak 2 (P2) ($P = .004$), and downslope of P2 ($P = .006$) distinguished the normal group from the keratoconus groups. The CRF, downslope of P2 derived from upper 50% of applanation peak ($P = .035$), dslope1 ($P = .014$), and upslope of P1 ($P = .008$) distinguished the normal group from the forme fruste keratoconus group.

CONCLUSION: Differences in multiple biomechanical waveform parameters can differentiate between healthy and diseased conditions and might improve early diagnosis of keratoconus and forme fruste keratoconus.

Financial Disclosure: No author has a financial or proprietary interest in any material or method mentioned.

J Cataract Refract Surg 2015; 41:2196–2204 © 2015 ASCRS and ESCRS

Laser in situ keratomileusis (LASIK) is the most frequently performed refractive surgery procedure due to outstanding postoperative uncorrected visual acuity and rapid recovery. However, corneal ectasia is still a dreaded complication following LASIK and

photorefractive keratectomy (PRK).^{1–3} Eyes with mild manifestations of keratoconus termed *forme fruste*, *suspect*, or *subclinical keratoconus* (hereafter termed *forme fruste keratoconus*) might not be detectable using even the most sophisticated topographic

and tomographic analyses in the early stages of the disease.² Keratoconus is a progressive disease, so it is important for refractive surgeons to be able to distinguish healthy corneas from keratoconic and forme fruste keratoconic corneas, particularly in typical younger populations who present for refractive surgery screening^{3,4}; otherwise, surgery in such eyes can lead to progressive ectasia and significant vision loss.⁵⁻⁷ In addition, new treatments using collagen crosslinking offer the potential to halt the progression of keratoconus, increasing the importance of early detection.⁸

It is well accepted that keratoconic corneas have abnormal properties, including their corneal resistance factor (CRF) and corneal hysteresis (CH).⁹⁻¹⁶ The Ocular Response Analyzer 2 (version 4.01, Reichert Technologies) used in this study is a biomechanical waveform analyzer, the second generation of a noninvasive and noncontact dynamic bidirectional applanation device that is commonly used to measure the biomechanical properties of the cornea. The system uses an air pressure pulse to produce inward and outward movement of the central cornea from which biomechanical waveform information is obtained. Briefly, an air puff deflects the cornea from its original shape through a first applanation and into slight concavity. The air puff progressively decreases, and the cornea passes through a second applanated state before returning to its original convex shape. During the corneal deformation process, an infrared light source reflects off the cornea and is measured by a detector. The intensity of the detected light depends on the shape of the cornea—a curved shape results in a lower intensity signal and a flat shape results in a higher intensity signal. Information from the optical system is recorded, analyzed, and presented as a corneal deformation signal.⁹ The CH, CRF, and the other 37 waveform parameters available on the second-generation dynamic bidirectional applanation device are not true biomechanical descriptors but

might assist the clinician in distinguishing normal from abnormal corneal viscoelastic conditions.

Biomechanics examination is a rapid dynamic measurement independent of topography. Studies have shown that a combination of the second-generation dynamic bidirectional applanation device and topography can improve the ability to diagnose forme fruste keratoconus.^{10,11} A study by Hallahan et al.¹² used the first-generation dynamic bidirectional applanation device to elucidate parameters that are significantly different between normal eyes and keratoconic eyes. Whereas the signals from the first-generation device can give valuable information, that platform still has some limitations in its ability to identify early keratoconus,¹³ due in part to long acquisition times, suboptimum accuracy, and reproducibility. The second-generation dynamic bidirectional applanation device platform allows significantly faster data acquisition than the first-generation device because of faster pupil tracking. This is due to improvements in the optical and mechanical hardware.^A

This study sought to determine the most sensitive and specific metrics for the discrimination between normal, forme fruste keratoconic, and keratoconic corneas using the second-generation of the dynamic bidirectional applanation device. To our knowledge, this is the first study to examine the difference in corneal biomechanical waveform parameters between keratoconic, forme fruste keratoconic, and normal corneas using the second-generation dynamic bidirectional applanation device.

PATIENTS AND METHODS

This retrospective chart review study was performed at the UCLA Laser Refractive Center and Contact Lens Department, Jules Stein Eye Institute, David Geffen School of Medicine at UCLA, from May 2013 to November 2013. Participants were selected from patients who presented to the clinic for refractive surgery screening or for keratoconus evaluation. Data from keratoconic, forme fruste keratoconic, and normal eyes were recorded. The study was approved by the Institutional Review Board at the University of California, Los Angeles, and followed the tenets of the Declaration of Helsinki.

Patients had a comprehensive ophthalmologic examination, including medical history; corrected visual acuity; slitlamp examination to identify the presence of Fleischer ring, Vogt striae, and corneal scarring characteristic of keratoconus; and a funduscopic examination. In addition, the patients had examinations using a scanning-slit corneal topographer (Orbscan IIz, Bausch & Lomb), the second-generation dynamic bidirectional applanation device, and a rotating dual Scheimpflug system (Galilei G2, version 5.0, Ziemer Ophthalmic Systems AG). All measurements were taken during the same visit. Only high-quality dynamic bidirectional applanation device readings were accepted for the study, as determined by consistency of measurements. All diagnoses were made by the same experienced corneal and refractive surgeon (D.R.H.).

Submitted: November 2, 2014.

Final revision submitted: March 19, 2015.

Accepted: March 21, 2015.

From the Refractive Center (Zhang), the 3rd Hospital of Dalian, Dalian Medical University, China; the UCLA Laser Refractive Center (Hamilton), Jules Stein Eye Institute (Tannan, Phan), David Geffen School of Medicine at the University of California (Danesh), and the Department of Biostatistics (Yu), UCLA Fielding School of Public Health, Los Angeles, California, USA.

Corresponding author: D. Rex Hamilton, MD, MS, UCLA Laser Refractive Center, Jules Stein Eye Institute, 200 Stein Plaza, Room 1-340, Los Angeles, California 90095, USA. E-mail: hamilton@jsei.ucla.edu.

Table 1. Second-generation dynamic bidirectional applanation device parameters.

| Number* | Name | Description |
|---------|----------|--|
| 1 | CH | Corneal hysteresis. Represents the corneal viscoelastic damping and reflects the capacity of corneal tissue to absorb and dissipate energy. |
| 2 | CRF | Corneal resistance factor. Calculated using a proprietary algorithm; is an indicator of overall corneal resistance. |
| 3 | IOPg | Goldmann-correlated intraocular pressure. The mean of the 2 applanation air pressure values (P1 and P2); correlates with Goldmann tonometry results. |
| 4 | IOPcc | Corneal-compensated intraocular pressure. Uses the corneal hysteresis to determine an intraocular pressure value that is less affected by corneal properties, such as central corneal thickness. |
| 5 | aindex | Degree of "nonmonotonicity" of rising and falling edges of peak1 (normalized by area). |
| 6 | bindex | Degree of "nonmonotonicity" of rising and falling edges of peak2 (normalized by area). |
| 7 | p1area | Area of peak1 (sum of values). |
| 8 | p2area | Area of peak2 (sum of values). |
| 9 | aspect1 | Aspect ratio of peak1 (height/width). |
| 10 | aspect2 | Aspect ratio of peak2 (height/width). |
| 11 | uslope1 | Upslope of peak1 (base to peak value of peak1). |
| 12 | uslope2 | Upslope of peak2 (base to peak value of peak2) (downslope in real time of peak2). |
| 13 | dslope1 | Downslope of peak1 (base to peak value of peak1). |
| 14 | dslope2 | Downslope of peak2 (base to peak value of peak2) (upslope in real time of peak2). |
| 15 | w1 | Width of peak1 at "base" of peak1 region. |
| 16 | w2 | Width of peak2 at "base" of peak2 region. |
| 17 | h1 | Height of peak1 (from lowest to highest value in peak1 region). |
| 18 | h2 | Height of peak2 (from lowest to highest value in peak2 region). |
| 19 | dive1 | Absolute value of monotonic decrease on downslope part of peak1 starting at the peak value. |
| 20 | dive2 | Absolute value of monotonic decrease on downslope part of peak2 starting at the peak value (monotonic increase in real time for peak2). |
| 21 | path1 | Absolute value of path length around peak1. |
| 22 | path2 | Absolute value of path length around peak2. |
| 23 | mslew1 | Maximum single-step increase in rise of peak1. |
| 24 | mslew2 | Maximum single-step increase in rise of peak2. |
| 25 | slew1 | Aspect ratio of dive1 (value of dive divided by width of dive region). |
| 26 | slew2 | Aspect ratio of dive2 (value of dive divided by width of dive region). |
| 27 | aplh | High-frequency "noise" in region between peaks (normalized by product of average of peak heights multiplied by width of region). |
| 28 | p1area1 | Area of peak1 (sum of values). |
| 29 | p2area1 | Area of peak2 (sum of values). |
| 30 | aspect11 | Aspect ratio of peak1 (height/width). |
| 31 | aspect21 | Aspect ratio of peak2 (height/width). |
| 32 | uslope11 | Upslope of peak1 (base to peak value of peak1). |
| 33 | uslope21 | Upslope of peak2 (base to peak value of peak2) (downslope in real time of peak2). |
| 34 | dslope11 | Downslope of peak1 (base to peak value of peak1). |
| 35 | dslope21 | Downslope of peak2 (base to peak value of peak2) (upslope in real time of peak2). |
| 36 | w11 | Width of peak1 at "base" of peak1 region. |
| 37 | w21 | Width of peak2 at "base" of peak2 region. |
| 38 | h11 | Height of peak1 (from lowest to highest value in peak1 region). |
| 39 | h21 | Height of peak2 (from lowest to highest value in peak2 region). |
| 40 | path11 | Absolute value of path length around peak1. |
| 41 | path21 | Absolute value of path length around peak2. |

*Parameters 5–27 are derived from the upper 75% of the applanation peak (defined on "baseline subtracted" signal). The second applanation region is "time reversed" so that upslope (uslope notation) of peak2 is actually a "downslope" (dslope notation) in real time. Parameters 28–41 have same descriptions as parameters 5–27 except they are derived from the upper 50% of the applanation peak

Topographically abnormal eyes were divided into 2 groups according to their keratoconus severity score.¹⁷ The keratoconic group included eyes with a score of more than 3 and the forme fruste keratoconic group contained eyes with a score of less than 3. Normal eyes were selected

from candidates who passed refractive surgery screening and were scheduled for LASIK. Scanning-slit corneal topography and rotating dual Scheimpflug system studies were obtained for all patients to confirm the keratoconus severity scoring.

Table 2. Demographics in the normal and keratoconus study groups.

| Characteristic | Study Group | | P Value |
|----------------|------------------|----------------------|----------------------|
| | Normal (n = 249) | Keratoconus (n = 68) | |
| Age (y) | | | < .0001* |
| Mean \pm SD | 36.3 \pm 12.8 | 45.6 \pm 14.5 | |
| Median | 32.0 | 49.0 | |
| Range | 18.0, 77.0 | 18.0, 71.0 | |
| Sex, n (%) | | | < .0009 [†] |
| Men | 123 (49) | 49 (72) | |
| Women | 126 (51) | 19 (28) | |
| Race, n (%) | | | .76 [‡] |
| White | 142 (68) | 41 (65) | |
| Other | 67 (32) | 22 (35) | |

t* test[†]Fisher exact test[‡]White versus all other race categories combinedTable 3.** Demographics in the normal and forme fruste keratoconus study groups.

| Characteristic | Study Group | | P Value |
|----------------|------------------|-----------------------------------|-------------------|
| | Normal (n = 249) | Forme Fruste Keratoconus (n = 64) | |
| Age (y) | | | < .0001* |
| Mean \pm SD | 36.3 \pm 12.8 | 47.3 \pm 17.1 | |
| Median | 32.0 | 49.0 | |
| Range | 18.0, 77.0 | 18.0, 74.0 | |
| Sex, n (%) | | | .012 [†] |
| Men | 123 (49) | 43 (67) | |
| Women | 126 (51) | 21 (33) | |
| Race, n (%) | | | 1.0 [‡] |
| White | 142 (68) | 37 (69) | |
| Other | 67 (32) | 17 (31) | |

**t* test[†]Fisher exact test[‡]White versus all other race categories combined

Central corneal thickness (CCT) was recorded from the rotating dual Scheimpflug system because this system has been shown to provide more accurate posterior corneal data than scanning-slit corneal topography.¹⁸ Age and sex were also recorded for each patient.

The second-generation dynamic bidirectional applanation device was used to obtain CH, CRF, and 37 biomechanical waveform parameters in keratoconic eyes, forme fruste keratoconic eyes, and normal eyes. These parameters describe various morphologic features of the corneal deformation signal (Table 1). The measurements were taken at least 3 times, and the measurement with the highest waveform score was used.

Statistical Analysis

All statistical analysis was performed using SAS statistical software (version 9.3, SAS Institute, Inc.). A 2-tailed *t* test was used to assess the difference in the mean of each dynamic bidirectional applanation device parameter between each

eye-disease group (keratoconus or forme fruste keratoconus) and the normal control group. A multivariable logistic regression model with a stepwise variable selection method was then used to select the dynamic bidirectional applanation device parameters that were most useful in distinguishing between each eye-disease group and the normal control group. The selected parameters for each eye disease (keratoconus or forme fruste keratoconus) were further adjusted by CCT, age, and sex in a final multivariable logistic regression model. Two receiver operating characteristic (ROC) curves were produced to demonstrate the ability to discriminate eyes with each eye disease from normal control eyes based on the corresponding final logistic regression model. The area under the ROC curve was also calculated. A *P* value less than 0.05 was considered statistically significant.

RESULTS

Tables 2 and 3 show the demographics in the 3 study groups. The study included 249 normal control eyes

Table 4. Comparison of waveform parameters between the normal group and the keratoconus group. Results are from a multivariate logistic regression model with stepwise variable selection after controlling for confounding factors.

| Parameter or Demographic | Study Group | | | | | | Mean Difference | Coefficient of Logistic Regression | P Value |
|--------------------------|------------------|--------|-------------|------------------|--------|--------------|-----------------|------------------------------------|---------|
| | Keratoconus | | | Normal | | | | | |
| | Mean \pm SD | Median | Range | Mean \pm SD | Median | Range | | | |
| CRF | 6.3 \pm 1.9 | 6 | 2.5, 11.7 | 10.2 \pm 1.7 | 9.9 | 5.9, 17.2 | 3.9 | -2.754 | .003 |
| h1 | 227.8 \pm 94.2 | 236 | 50.8, 423.4 | 402.7 \pm 91.6 | 408.6 | 203.1, 653.6 | 174.9 | -0.048 | .001 |
| dslope1 | 20.3 \pm 9.2 | 20.6 | 2.1, 40.3 | 29.1 \pm 8.1 | 28.8 | 9.6, 55.7 | 8.8 | 0.237 | .027 |
| uslope2 | 37.7 \pm 26.7 | 30.5 | 2.3, 131.6 | 65.1 \pm 29 | 61.5 | 9.2, 200.6 | 27.4 | 0.112 | .004 |
| dslope2 | 22.8 \pm 14 | 20.5 | 1.1, 71.1 | 23.9 \pm 10.5 | 22.6 | 3.4, 105 | 1.1 | 0.13 | .006 |
| Age | 45.6 \pm 14.5 | 49 | 16, 71 | 36.3 \pm 12.8 | 32 | 17, 77 | -9.3 | 0.106 | .026 |

CRF = corneal resistance factor; dslope1 = downslope of peak1 (base to peak value of peak1); dslope2 = downslope of peak2 (base to peak value of peak2) (upslope in real time of peak2); h1 = height of peak1 (from lowest to highest value in peak1 region); uslope2 = upslope of peak2 (base to peak value of peak2) (downslope in real time of peak2)

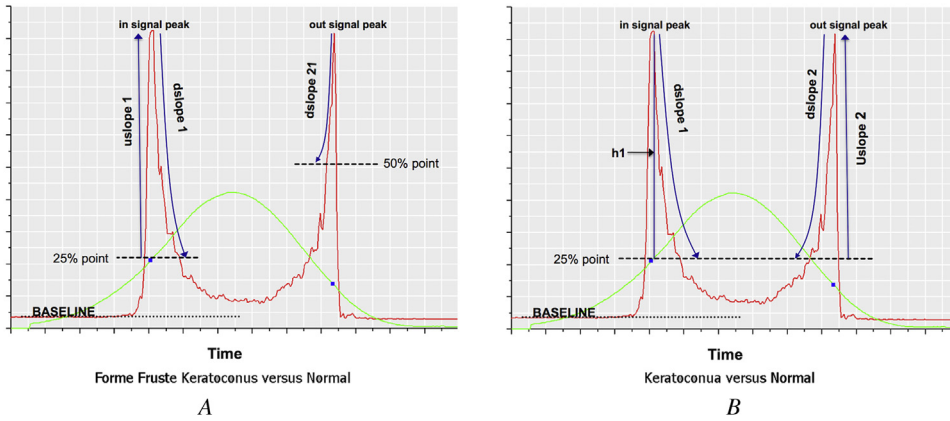


Figure 1. Corneal deformation signal waveforms demonstrate parameters with statistically significant differences between a manifest keratoconus cornea and a normal cornea (A) and a forme fruste keratoconus cornea and a normal cornea (B). (See Table 1 for a description of the parameters.)

of 127 patients, 68 keratoconic eyes of 50 patients, and 64 forme fruste keratoconic eyes of 47 patients. There was no statistically significant difference in race between the normal and keratoconus groups ($P = .76$) or the normal and forme fruste keratoconus groups ($P = 1.00$). There were statistically significant differences in age and sex between the normal and keratoconus groups ($P < .0001$ and $P = .0009$, respectively), and between the normal and forme fruste keratoconus groups ($P < .0001$ and $P = .012$, respectively). The mean CCT in normal, keratoconic, and forme fruste keratoconic eyes was $557.2 \mu\text{m} \pm 29.9$ (SD) (range 492.0 to $634.0 \mu\text{m}$), $474.3 \pm 66.0 \mu\text{m}$ (range 238.0 to $644.0 \mu\text{m}$; $P < .0001$ compared with normal), and $511.6 \pm 34.7 \mu\text{m}$ (range 356.0 to $589.0 \mu\text{m}$; $P < .0001$ compared with normal), respectively.

For the separation of keratoconic eyes from normal eyes, the logistic regression model with stepwise variable selection chose the following 6 parameters from the 41 total parameters in order of significance: CRF ($P < .0001$), height of peak 1(P1) (h1) ($P < .0001$), downslope of P1 (dslope1) ($P < .0001$), upslope of peak 2 (P2) (uslope2) ($P = .0003$), downslope of P2 (dslope2) ($P = .002$), and CH ($P = .005$). The area

under the ROC curve for this model was 0.990. After statistically adjusting for age ($P = .026$), male sex ($P = .21$), and CCT ($P = .14$), the CH mean difference lost statistical significance ($P = .14$). However, the difference between the means of CRF ($P = .003$) and 4 waveform parameters remained statistically significant (Table 4). (See Figures 1 and 2 for a description of the parameters.) The area under the ROC curve for this model using CRF and the 4 waveform parameters improved to 0.991 (Figure 3).

For the separation of forme fruste keratoconic eyes from normal eyes, the logistic regression model with stepwise variable selection chose the following 5 parameters from the 41 total parameters in order of statistical significance: CRF ($P < .0001$), downslope of P2 derived from upper 50% of applanation peak (dslope21) ($P = .006$), dslope1 ($P = .0016$), maximum single-step increase in the rise of P2 (mslew2) ($P = .027$), and upslope of P1 (uslope1) ($P = .038$). The area under the ROC curve for this model was 0.904. After statistically adjusting for age ($P = .0006$), male sex ($P = .054$), and CCT ($P = .006$), all parameters including CRF ($P < .0001$) remained statistically significant (Table 5) except for mslew2 ($P = .20$).

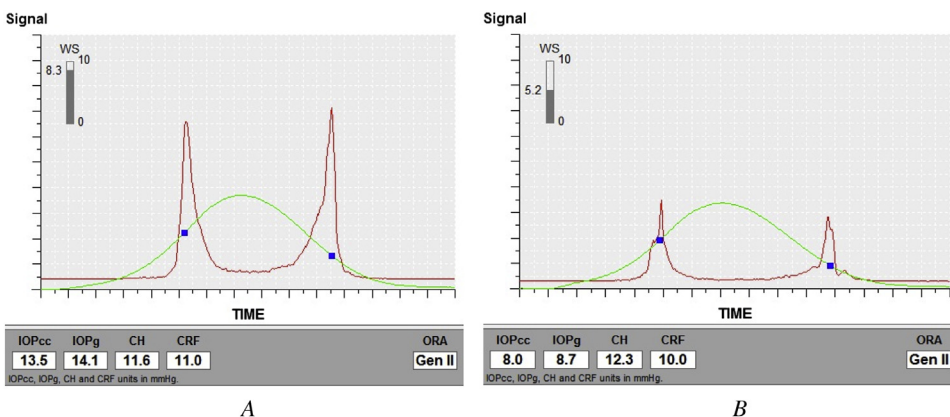


Figure 2. A signal waveform in a normal cornea (A) compared with a waveform in a forme fruste keratoconic cornea (B) shows a significantly lower CRF and uslope1 and a higher dslope 21 and dslope1. (See Table 1 for a description of the parameters.)

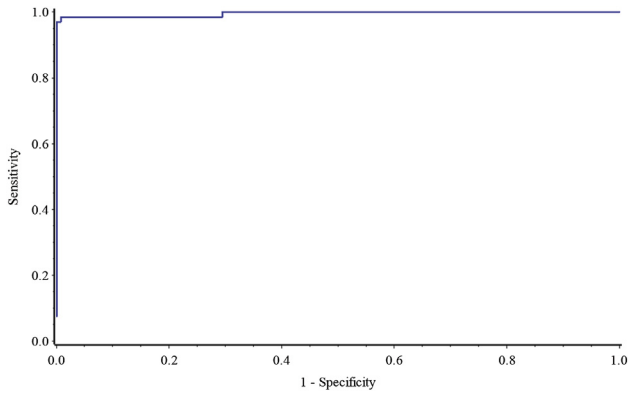


Figure 3. Based on a model with parameters CRF ($P = .003$), $h1$ ($P = .001$), $dslope1$ ($P = .037$), $uslope2$ ($P = .004$), $dslope2$ ($P = .006$), CH ($P = .14$), age ($P = .026$), male sex ($P = .21$), and CCT ($P = .14$), the area under the ROC curve was 0.991.

(See Figures 1 and 4 for a description of the parameters.) The area under the ROC curve for this model using CRF and the 3 waveform parameters was 0.931 (Figure 5).

DISCUSSION

To our knowledge, this study is the first study designed to evaluate the corneal signal waveforms between keratoconic, forme fruste keratoconic, and normal eyes using the second-generation dynamic bidirectional applanation device. The purpose of this study was to compare the difference in corneal biomechanical waveform parameters between keratoconic, forme fruste keratoconic, and normal corneas after controlling for potentially confounding factors.

The detection of keratoconus and forme fruste keratoconus is essential when screening patients for LASIK and PRK. Although, sophisticated tomographic analysis has improved significantly over the

past 10 years, forme fruste keratoconus is still challenging to detect even using the most advanced tomographic technologies. Muftuoglu et al.¹⁹ found that as sole parameters, both back difference corneal elevation and posterior corneal elevation had limited sensitivity and specificity to differentiate between forme fruste keratoconic eyes and normal control eyes. In 2015,²⁰ an expert panel on the diagnosis and management of keratoconus reached a consensus regarding the definition and diagnosis of keratoconus. It was agreed that there is currently no single modality or classification system that can adequately define keratoconus. Although tomography is considered to be the best and most widely accessible diagnostic tool at this time, tomographic analysis alone is not sufficient to detect early keratoconus. Although the findings of abnormal posterior elevation, abnormal corneal thickness distribution, and clinical noninflammatory corneal thickening are all required to make a diagnosis of keratoconus, subtle changes in these elements may not be detected by tomography.²⁰ Ultimately, there might be cases in which there are no detectable tomographic abnormalities despite the eye being diseased. The second-generation dynamic bidirectional applanation device can assist in this setting by providing information on the disease state separate from corneal shape. A thin cornea and young age are also considered risk factors for eyes developing ectasia after LASIK.³ However, there have been recent reports of moderate keratoconus with thick corneas and keratoconus onset after age 50.^{21,22}

The idea has been accepted and reinforced that assessing corneal biomechanics can be a useful adjunctive tool in the diagnosis, development, and/or progression of keratoconus.^{10-13,23} Several previous studies examined the difference in dynamic bidirectional applanation device corneal deformation signal waveform parameters between normal corneas and

Table 5. Comparison of waveform parameters between the normal group and the forme fruste keratoconus group. Results are from a multivariate logistic regression model with stepwise variable selection after controlling for confounding factors.

| Parameter or Demographic | Study Group | | | | | | Mean Difference | Coefficient of Logistic Regression | P Value |
|--------------------------|--------------------------|--------|-------------|------------------|--------|--------------|-----------------|------------------------------------|---------|
| | Forme Fruste Keratoconus | | | Normal | | | | | |
| | Mean \pm SD | Median | Range | Mean \pm SD | Median | Range | | | |
| CRF | 7.8 \pm 1.4 | 7.8 | 4.6, 11.7 | 10.2 \pm 1.7 | 9.9 | 5.9, 17.2 | 2.4 | -0.872 | <.0001 |
| dslope21 | 42.8 \pm 20.9 | 39 | 8.4, 108.3 | 402.7 \pm 91.6 | 408.6 | 203.1, 653.6 | 359.9 | 0.03 | .035 |
| uslope1 | 58.4 \pm 22.1 | 57 | 20.3, 131.4 | 29.1 \pm 8.1 | 28.8 | 9.6, 55.7 | 29.3 | -0.033 | .008 |
| dslope1 | 33.2 \pm 9.8 | 33.4 | 10.2, 60 | 65.1 \pm 29 | 61.5 | 9.2, 200.6 | 31.9 | 0.077 | .014 |
| Age | 47.3 \pm 17.1 | 49 | 15, 74 | 23.9 \pm 10.5 | 22.6 | 3.4, 105 | 23.4 | 0.043 | .0006 |

CRF = corneal resistance factor; dslope1 = downslope of peak1 (base to peak value of peak1); dslope21 = downslope of peak2 (base to peak value of peak2) (upslope in real time of peak2); uslope1 = upslope of peak1 (base to peak value of peak1)

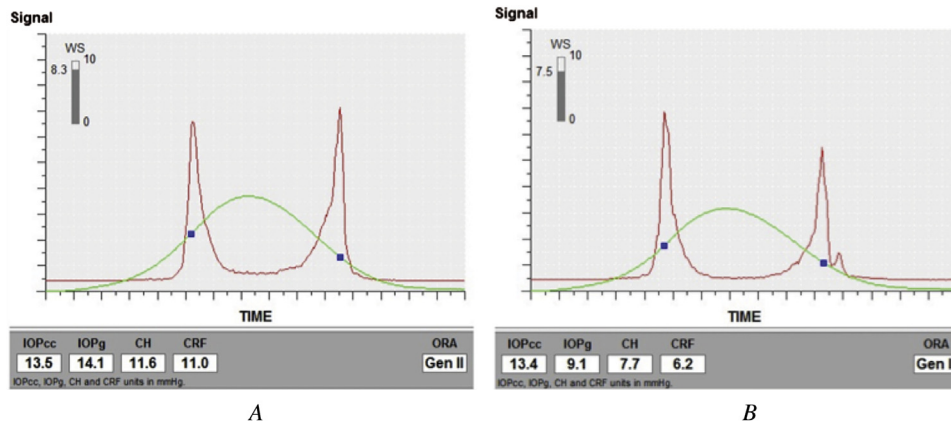


Figure 4. A signal waveform in a normal cornea (A) compared with a waveform in a manifest keratoconic cornea (B) demonstrates a significantly lower CRF, h1, dslope1, uslope2, and dslope2. (See Table 1 for a description of the parameters.)

diseased corneas.^{11,12,23} There is a significant overlap in the distribution of CH and CRF values among normal and diseased groups.^{13,23} In previous studies, the CRF has been considered a parameter most related to corneal elasticity, a “marker” for the keratoconus disease state.²⁴ In our study, univariate analysis showed a significant lower mean CRF in both keratoconus and forme fruste keratoconus. Although CH and CRF are useful as adjunctive clinical parameters when using other diagnostic tools, they cannot be used alone.^{13,25}

Patient age and sex have effects on both CH and CRF. In addition, the CRF has a strong positive correlation with the CCT.^{14,15} Therefore CCT, age, and sex should be considered confounding factors in studies of corneal biomechanics. Multivariate analysis in our study showed that after controlling for CCT, age, and sex, the difference in the CRF was still statistically significant between the normal group and the keratoconus and forme fruste keratoconus groups ($P = .003$ and $P < .0001$, respectively) whereas the

difference in CH was no longer significant. Our conclusion is similar to that of Galletti et al.,²⁶ who found that true positive rate for the CRF in eyes with keratoconus with normal topography was 84% and the CRF was better than CH for detecting keratoconic corneas once the effect of the CCT on dynamic bidirectional applanation device measurements was considered, even for topographically normal fellow eyes of patients with keratoconus. The loss of significance of the CH difference likely relates to a lower sensitivity and specificity in keratoconus detection compared with the CRF.

In our study, multivariate logistic regression model analysis with confounding factors control showed that besides the CRF, the parameters h1, dslope1, uslope2, and dslope2 were statistically different between the normal group and the keratoconus groups and the parameters dslope21, uslope1, and dslope1 were statistically significant between the normal group and the forme fruste keratoconus groups. Based on a model with these significant parameters, the area under the curve (AUC) for the ROC curve was 0.991 and 0.931 in the normal group compared with the keratoconus group and the forme fruste keratoconus group, respectively. Ventura et al.¹⁶ analyzed 136 eyes with normal corneas and 68 eyes with keratoconus and found 4 dynamic bidirectional applanation device parameters significant for separating the groups (p1area, p1area1, p2area, and p2area1), yielding an AUC for the ROC curve of 0.978 when using all 4 parameters together. The AUC using 5 parameters in our study (0.991) is higher than the AUC with all parameters (0.978) in the Ventura et al. study.¹⁶ Reasons for this might include the use of the second-generation dynamic bidirectional applanation device in our study, which appears to have better reproducibility and a better signal-to-noise ratio than the first-generation device. The second-generation device has a smaller overlap in parameter values between groups; in our

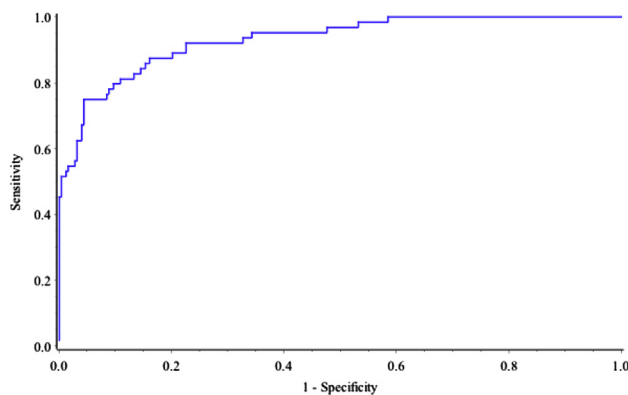


Figure 5. The ROC curve for forme fruste keratoconic eyes versus normal eyes based on the model with parameters CRF ($P < .0001$), dslope21 ($P = .035$), uslope1 ($P = .008$), dslope1 ($P = .014$), mslew2 ($P = .20$), age ($P = .0006$), male sex ($P = .054$), and CCT ($P = .006$). The area under the ROC curve was 0.931.

study, even after adjusting for CCT, the CRF still had a statistically significant difference between the normal group and the keratoconus group ($P = .003$) and the forme fruste keratoconus group ($P < .0001$). Another reason for a difference in results might be how forme fruste keratoconus was defined in the 2 studies. In our study, we used the method from the Collaborative Longitudinal Evaluation of Keratoconus study group¹⁷ to grade the severity of the forme fruste keratoconus. Ventura et al.¹⁶ used only central keratometry to stratify severity of keratoconus.

Zarei-Ghanavati et al.¹¹ showed that dslope1, uslope1, and P1 area were useful biomechanical waveform parameters to differentiate between healthy post-LASIK and keratoconic corneas. It is interesting that our study of normal corneas without previous LASIK found the same parameters dslope1 and uslope1 as well as related parameters dslope2, dslope21, and uslope2 to be the most important in distinguishing normal corneas from keratoconic corneas.

Our study results must be evaluated considering its limitations. We did not independently verify the model found in this study with an additional population of normal, forme fruste keratoconic, and keratoconic corneas to confirm its value. In addition, we do not currently have a keratoconus match index, whose development using these new parameters would allow for more efficient identification of suspect keratoconic corneas. Once significant parameters are identified on the second-generation dynamic bidirectional applanation device, a new keratoconus match index specific to the second-generation dynamic bidirectional applanation device can be developed. The parameters on the first-generation dynamic bidirectional applanation device do not necessarily translate to the second-generation dynamic bidirectional applanation device because of the latter's faster data acquisition and improved optical and mechanical hardware.^A The 7 parameters used to develop the keratoconus match index for the first-generation dynamic bidirectional applanation device might not be the same parameters that would be best to use for a keratoconus match index on the second-generation device.

This study using the second-generation dynamic bidirectional applanation device found several waveform parameters useful for discriminating between keratoconic, forme fruste keratoconic, and normal corneas. The ROC curves analyzing the sensitivity and specificity of separating normal eyes from both forme fruste keratoconic and keratoconic eyes showed excellent discrimination. This study suggests that the second-generation dynamic bidirectional applanation device might be useful as an adjunct to corneal topography and tomography in the identification of early keratoconus and forme fruste keratoconus.

WHAT WAS KNOWN

- The CRF and CH are lower in corneas with forme fruste keratoconus or manifest keratoconus than in normal corneas, although there is a significant overlap in the distribution of these 2 factors among normal corneas and diseased corneas, as measured by the first-generation dynamic bidirectional applanation device.
- The first-generation dynamic bidirectional applanation device parameter P1area has been documented in the literature to be a useful parameter to separate cases of mild keratoconus and healthy corneas with less overlap than CH and the CRF.
- The CRF, h1, dslope1, uslope2, and dslope2 are statistically different between the normal group and the keratoconus group. The CRF, dslope21, dslope1, and uslope1 are statistically different between the normal group and the forme fruste keratoconus group.

WHAT THIS PAPER ADDS

- Multiple corneal biomechanical waveform parameters and the CRF were significantly different when comparing normal corneas with forme fruste keratoconic and manifest keratoconic corneas after using multivariable logistic regression to control for potential confounding factors.

REFERENCES

1. Seiler T, Koufala K, Richter G. Iatrogenic keratectasia after laser in situ keratomileusis. *J Refract Surg* 1998; 14:312–317
2. Malecaze F, Couillet J, Calvas P, Fournié P, Arné J-L, Brodaty C. Corneal ectasia after photorefractive keratectomy for low myopia. *Ophthalmology* 2006; 113:742–746
3. Chan CCK, Hodge C, Sutton G. External analysis of the Randleman Ectasia Risk Factor Score System: a review of 36 cases of post LASIK ectasia. *Clin Exp Ophthalmol* 2010; 38:335–340
4. Randleman JB, Woodward M, Lynn MJ, Stulting RD. Risk assessment for ectasia after corneal refractive surgery. *Ophthalmology* 2008; 115:37–50
5. Guirao A. Theoretical elastic response of the cornea to refractive surgery: risk factors for keratectasia. *J Refract Surg* 2005; 21:176–185
6. Chiang RK, Park AJ, Rapuano CJ, Cohen EJ. Bilateral keratoconus after LASIK in a keratoconus patient. *Eye Contact Lens* 2003; 29:90–92
7. Seiler T, Quurke AW. Iatrogenic keratectasia after LASIK in a case of forme fruste keratoconus. *J Cataract Refract Surg* 1998; 24:1007–1009
8. Ghanem RG, Santhiago MR, Berti T, Netto MV, Ghanem VC. Topographic, corneal wavefront, and refractive outcomes 2 years after collagen crosslinking for progressive keratoconus. *Cornea* 2014; 33:43–48
9. Luce DA. Determining in vivo biomechanical properties of the cornea with an ocular response analyzer. *J Cataract Refract Surg* 2005; 31:156–162
10. Wolffsohn JS, Safeen S, Shah S, Laiquzzaman M. Changes of corneal biomechanics with keratoconus. *Cornea* 2012; 31:849–854

11. Ghanavati S, Ramirez-Miranda A, Yu F, Hamilton DR. Corneal deformation signal waveform analysis in keratoconic versus post-femtosecond laser in situ keratomileusis eyes after statistical correction for potentially confounding factors. *J Cataract Refract Surg* 2012; 38:607–614
12. Hallahan KM, Sinha Roy A, Ambrosio R Jr, Salomao M, Dupps WJ Jr. Discriminant value of custom Ocular Response Analyzer waveform derivatives in keratoconus. *Ophthalmology* 2014; 121:459–468
13. Johnson RD, Nguyen MT, Lee N, Hamilton DR. Corneal biomechanical properties in normal, forme fruste keratoconus, and manifest keratoconus after statistical correction for potentially confounding factors. *Cornea* 2011; 30:516–523
14. Touboul D, Roberts C, Kérautret J, Garra C, Maurice-Tison S, Saubusse E, Colin J. Correlations between corneal hysteresis, intraocular pressure, and corneal central pachymetry. *J Cataract Refract Surg* 2008; 34:616–622
15. Kamiya K, Shimizu K, Ohmoto F. Effect of aging on corneal biomechanical parameters using the Ocular Response Analyzer. *J Refract Surg* 2009; 25:888–893
16. Ventura BV, Machado AP, Ambrósio R Jr, Ribeiro G, Araújo LN, Luz A, Lyra JM. Analysis of waveform-derived ORA parameters in early forms of keratoconus and normal corneas. *J Refract Surg* 2013; 29:637–643
17. McMahon TT, Szczotka-Flynn L, Barr JT, Anderson RJ, Slaughter ME, Lass JH, Iyengar SK; and the CLEK Study Group. A new method for grading the severity of keratoconus: the Keratoconus Severity Score (KSS). *Cornea* 2006; 25:794–800
18. Sy ME, Ramirez-Miranda A, Zarei-Ghanavati S, Engle J, Danesh J, Hamilton DR. Comparison of posterior corneal imaging before and after LASIK using dual rotating Scheimpflug and scanning slit-beam corneal tomography systems. *J Refract Surg* 2013; 29:96–101
19. Muftuoglu O, Ayar O, Ozulken K, Ozyol E, Akinci A. Posterior corneal elevation and back difference corneal elevation in diagnosing forme fruste keratoconus in the fellow eyes of unilateral keratoconus patients. *J Cataract Refract Surg* 2013; 39:1348–1357
20. Gomes JAP, Tan D, Rapuano CJ, Belin MW, Ambrósio R Jr, Guell JL, Malecaze F, Nishida K, Sangwan VS, the Group of Panelists for the Global Delphi Panel of Keratoconus and Ectatic Diseases. Global consensus on keratoconus and ectatic diseases. *Cornea* 2015; 34:359–369
21. Berti TB, Ghanem VC, Ghanem RC, Binder PS. Moderate keratoconus with thick corneas. *J Refract Surg* 2013; 29:430–435
22. Tenkman LR, Price MO, Price FW Jr. Keratoconus onset after age 50. *J Refract Surg* 2012; 28:436–438
23. Mikielewicz M, Kotliar K, Barraquer RI, Michael R. Air-pulse corneal applanation signal curve parameters for the characterization of keratoconus. *Br J Ophthalmol* 2011; 95:793–798
24. Avetisov SE, Novikov IA, Bubnova IA, Antonov AA, Siplivyi VI. Determination of corneal elasticity coefficient using the ORA database. *J Refract Surg* 2010; 26:520–524
25. Fontes BM, Ambrósio R Jr, Jardim D, Velarde GC, Nosé W. Corneal biomechanical metrics and anterior segment parameters in mild keratoconus. *Ophthalmology* 2010; 117:673–679
26. Galletti JG, Pfoertner T, Bonthoux FF. Improved keratoconus detection by ocular response analyzer testing after consideration of corneal thickness as a confounding factor. *J Refract Surg* 2012; 28:202–208

OTHER CITED MATERIAL

- A. Dave Taylor, Reichert Technologies, personal communication, February 18, 2015